RSC Advances

ROYAL SOCIETY OF CHEMISTRY

www.rsc.org/advances

RSC Advances

RSCPublishing

ARTICLE

Water desalination through armchair carbon nanotubes: A molecular dynamics study

Cite this: DOI: 10.1039/xoxxoooooox

J. Azamat*, J.J. Sardroodi, A. Rastkar

Received ooth January 2014,
Accepted ooth January 2014

DOI: 10.1039/xoxxoooooox

www.rsc.org/

In this paper, molecular dynamics simulations were performed to study desalination performance of armchair carbon nanotubes (CNTs). The studied systems included the (7, 7) and (8, 8) CNTs embedded in a silicon nitride membrane immersed in an aqueous ionic solution. For desalinating water, an external electrical field was applied to the systems along the axis of nanotubes. The results indicated that the (7, 7) and (8, 8) CNTs were exclusively selective to ions. The (7, 7) CNT selectively separated sodium ions from aqueous solution. In contrast, the (8, 8) CNT selectively separated chlorine ions. CNTs ion selectivity is justified by calculating the potential of mean force for each ion in the related system. Also, the results were confirmed using the following simulated properties: ion current, retention time of ions, transport rate for water molecules, the average density of water inside the CNTs, and the radial distribution functions of ions-water. Based on the findings of this study, the studied systems can be recommended as a model for the desalination of water.

1. Introduction

Water is the most important component of world and it has a critical role in the ecosystem of the earth. Water use has been increasing at a rate more than that of population growth. Recently, clean water is not available in some parts of the world and many people in the world do not have access to clean water due to natural disasters, war and weak infrastructure purified water. Contamination has diminished the quality of water resources. [1-3]

Water resources supply the required water for different types of use. Various resources are used for the production of water around the world. Saltwater is considered as one important type of water resource. When the concentration of dissolved salts increases significantly, the water will become saltwater or saline water. Saltwater resources are very useful for humans and they also save the environment from harm. Desalinated water is separated from freshwater and saline water. Oceans and seawaters are the main resources of saltwater. Water desalination technology has changed and a new instance of nanotechnology is used. However, the lack of access to clean water has called for the development and use of new technologies. The most important challenge in treating contaminated water is the cost of the required methods. It can be maintained that selecting the proper nanostructures for constructing membranes will play an important role in the effectiveness of water-desalination processes. The selective transport of ions by means of nanostructure membranes is of high significance and is regarded as a hot issue in many related research areas. The use of nanomaterials in general and carbon nanotubes (CNTs) in particular are considered as one of the controversial arguments in this area. CNTs with their nano scale diameters can have potential applications in the desalination process.

[a]Molecular Simulations Lab., Azarbaijan Shahid Madani University, Tabriz, Iran; E-mail:jafar.azamat@azaruniv.edu;jafar.azamat@yahoo.com

They have cylindrical nanostructure and are conceptualized by wrapping graphene. [4] CNTs are characterized by a pair of indexes (n, m). The n and m indexes are the number of unit vectors of graphene sheet. Based on the values of these two indexes, there are three types of CNTs; zigzag (m =0), armchair (n =m) and chiral (n ≠m). The inner diameter of a CNT can be computed from the Eq(1).[5]:

$$d_{in} = (\frac{a}{\pi})\sqrt{(n^2 + m^2 + nm) - 2r_c} \qquad (1)$$

where d_{in}, a and r_c stand for inner diameter of nanotubes, graphene lattice parameter (2.46 Å) and van der Waal's radius of a carbon atom (1.7 Å), respectively.

Since the discovery of CNTs in 1991, [6] they have been studied extensively.[7-9] Due to their special properties, CNTs have attracted researchers' attention. The electronic structure of a CNT can be both semiconductor and metallic. [10, 11] Since CNTs provide low energy solution for water treatment, they are considered as useful and efficient nanomaterials for desalinating water in membrane industries. Diameter of nanotubes is regarded as an effective parameter in transporting ions. It has been shown that the small diameter of CNTs rejects ions and only water molecules can be passed through the nanotubes.[5, 12, 13] Some studies have experimentally indicated that water molecules can enter CNTs.[14] It can be mentioned that further studies of CNTs can reveal potential applications of them. Lately, there has been growing interest in studying the mechanisms of ion transport. A variety of nanotubes has been suggested as membranes for ion separation.[15-19] To date, researchers have designed and fabricated ion-selective nanotubes constructed from carbon atoms. [20-28]

In this study, the researchers used the (7, 7) and (8, 8) CNTs by molecular dynamics (MD) simulation to study the selective removal

of sodium and chloride ions by applied an external electrical field. In the other work,[29] ab initio MD was utilized to investigate water ionization rather than electrical field. MD simulation technique can investigate the microscopic details of desalination phenomenon. Design, production and scale up of various processes can be simulated by this method.

2. Computational method and details

As mentioned above, (7, 7) and (8, 8) CNTs were selected in the present study. The optimized geometries of the CNTs were done at the B3LYP level of theory using 6-311G (2d, 2p) basis sets using GAMESS-US package. [30]

MD calculations were performed using the NAMD molecular dynamics package developed at the University of Illinois at Urbana-Champaign [31] with a 1 fs time step and it was visualized by VMD, a visualization package available from UIUC [32] as previous works [33-36]. The effective potential energy (U_{eff}) of intermolecular interactions was given by the sum of Lennard-Jones 12-6 (U_{vdw}) and coulomb (U_C) potentials for short-range and long-range interactions respectively, through Eq. (2).

$$U_{eff} = U_{vdw} + U_C = 4\sqrt{\varepsilon_i \varepsilon_j}\left[\left(\frac{(\sigma_i+\sigma_j)}{2r_{ij}}\right)^{12} - \left(\left(\frac{(\sigma_i+\sigma_j)}{2r_{ij}}\right)\right)^{6}\right] + \frac{q_i q_j}{4\pi\varepsilon_0 r_{ij}} \qquad (2)$$

where r_{ij} refers to the distance between the atoms i and j. ε_i and σ_i stand for the Lennard-Jones parameters which are related to atom i. q_i and q_j represent the partial charge assigned to atoms i and j. The short-range interactions parameters of CNT atoms were characterized by the 12-6 Lennard-Jones potential [37] through ε_{carbon}= 0.0607 kcal/mol, σ_{carbon}= 3.369 Å. All carbon atoms in the CNT are assumed to be electrically neutral and therefor without coulomb interactions.[38] The Lorentz-Berthelot combining rules were used for the cross interaction parameters between species, i.e.,

$$\varepsilon_{ij} = \sqrt{\varepsilon_i . \varepsilon_j} \quad \text{and} \qquad (3)$$

$$\sigma_{ij} = \frac{\sigma_i + \sigma_j}{2}$$

where ε_{ij} and σ_{ij} are regarded as the usual empirical Lennard-Jones parameters between i and j sites.

All analysis scripts were composed locally using both VMD and Tcl commands. The Particle Mesh Ewald algorithm [39] was used for electrostatic calculation. The MD domain consisted of a CNT fixed in a silicon nitride membrane, water molecules, and 0.5 M NaCl aqueous solution. (See Fig.1)

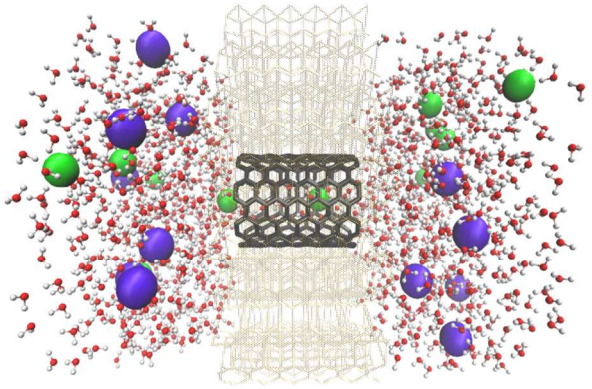

Fig.1 The (8, 8) CNT shown inside a silicon nitride membrane between two reservoirs containing water and ions (gray: silicon nitride membrane; black: CNT; violet: Na^+; green: Cl^-; red and white: water).

In experiments, nanotubes were often embedded in silicon nitride [40] or a polystyrene film. [41, 42] In MD simulations, nanotubes were embedded in a variety of matrices including silicon nitride, [43] lipid bilayers, [44] and graphene bilayers. [45, 46] The length of CNTs was 15 Å and their radii were 4.755 Å and 5.445 Å for the (7, 7) and (8, 8) CNTs, respectively. The simulation box for all runs was 3.5×4×5 nm^3. The system was first minimized for 1 ns, and then equilibrated with MD for 4 ns. An electrical field was used for all the systems which was defined through Eq. (4).

$$e_{field} = -23.0605492\frac{V}{l_z} \qquad (4)$$

where e_{field}, V and l_z stand for the applied electrical field (in $kcal.mol^{-1}.Å^{-1}.e^{-1}$), potential difference (in Volt) and size of the system along the z-axis (in Ångstrom), respectively.[47] The system was equilibrated for 1 ns under the constant temperature of 298 K. For the water molecules, was used from the intermolecular three point potential model (TIP3P) [48] and the CHARMM force field [49] was used for all simulations. The Lennard-Jones parameters for sodium and Chlorine were obtained from Joung et al.[50] Lennard-Jones parameters employed for atoms in this work are reported in Table 1.

Table1. Lennard-Jones parameters employed in this work.

Atom	Partial charges	σ (Å)	ε (kcal/mol)
Carbon	0	3.369	0.0607
Nitrogen	-0.5607	3.559	0.190
Silicon	0.7710	3.804	0.310
Sodium	+1.00	2.439	0.0874
Chlorine	-1.00	4.477	0.0356

The silicon nitride membrane and CNTs were restrained with a harmonic constraint while water molecules and ions were allowed to move freely. The ion current for the studied systems was computed using Eq. (5).

$$I = \frac{n.q}{\Delta T} \qquad (5)$$

where n is the average number of ions that pass the CNT, q is the charge of the ion and Δt is the simulation time.

The contrasting ion selectivity of CNTs can be explained by the potential of mean force (PMF). [51] The PMF of the specific ion moving through the nanotube was determined using umbrella sampling in which a harmonic biasing potential, i.e.,

$$(K_z / 2)(z - z_i)^2 \qquad (6)$$

This was applied to a test ion, where z refers to the axial coordinates of the ion defined from the centre of one of the pores, z_i denotes target ion positions, and K_z is corresponding force constants. The ions were moved through positions from -7.5 Å to 7.5 Å. in 0.5 Å increments and the z component held using a harmonic constraint of 12.5 kcal mol^{-1} $Å^{-2}$ whereas the ion was free to move radially. This harmonic constraint was chosen to give sufficient overlap between each window and its neighbours while constraining the ions to ensure sufficient sampling of the entire reaction coordinate. Prior to all simulations, the test ion(s) was held fixed for 10 ps to allow water to equilibrate around it. Each sampling window was run for 1

ns. The ion coordinates were obtained during each umbrella sampling run of 1ns, and the data were analysed using the weighted histogram analysis method [52] (WHAM), to obtain PMF.

3. Results and discussion

For investigating the desalination phenomenon, the researchers selected the MD simulations method which is considered to be an appropriate tool for the purpose of the study. The investigated system included 0.5 M NaCl aqueous solution and (7, 7) and (8, 8) CNTs. Also, the external electrical field was applied to examine the desalination process. Under the influence of this electrical field, a sodium or chlorine ion permeates from the appropriate CNT. In this study, included the following parameters were investigated:

- Ionic current
- Normalized transport rate of water with respect to the number of transported ions
- Hydrogen bonds inside the CNTs
- Average density of water inside the CNTs
- Ion retention time
- Ion-water radial distribution functions

Although the examined CNTs have a radius which is large enough to enter Na^+ and Cl^- ions, results of MD simulations indicated that the ions permeated through these nanotubes after applying the electrical field. The transportation directions of the two kinds of ions were different because the electric field was just in one direction; therefore the sodium and the chlorine were transported in opposite direction. The results of this study reveal that one Na^+ ion entered the (7, 7) CNT and was able to go through the entire length of the nanotube and get out of it. In contrast, none of the Cl^- ions were not able to even enter the (7, 7) CNT. In the case of (8, 8) CNT, the opposite phenomenon occurs.

The silicon nitride membrane atoms lied in the immediate neighbourhood of CNT's control the type of ions entering into CNT. This arises from the orientation of dipole moment of water molecules due to the electrostatic interactions between membrane atoms and oxygen or hydrogen atoms of water. The direction of dipole moment vector of water molecules orients to the walls of (7,7) CNT whiles toward the axis of (8,8) CNT. This different orientation is caused from membrane nitrogen and silicon atoms surrounding (7, 7) and (8, 8) CNTs respectively. At the absent of CNT, the considered ions are adsorbed in the pore inside membrane. The water desalination is a phenomenon dependent on both CNT diameter and the type of surrounding atoms belonging to the membrane.

The phenomenon of ion selectivity in the respective systems was examined by calculating the potentials of mean force (PMF); i.e., free energy profiles for a given ion as it was moved along the z axis of system. Fig. 2 represents PMF for the considered ions. As it can be observed from this Fig., there was an energy barrier in the (7, 7) CNT for Cl^- ions which inhibited the permeation of Cl^-. In the case of the (8, 8) CNT, there was energy barrier for Na^+ ions.

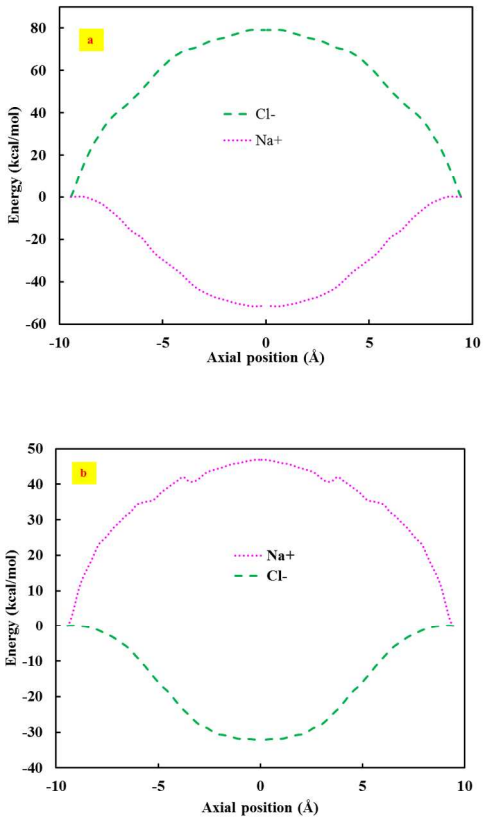

Fig.2 Potential of mean force for the Na^+ and Cl^- ions in the: (a) (7, 7) CNT; (b) (8, 8) CNT.

In the conducted simulations, the PMF increased at the pore openings and reached its maximum value at the pore centre inside the nanotube. This was due to the interactions between anion, CNT and silicon nitride membrane. This was in complete agreement with the results of the simulations. Simulation results acknowledged that since PMF had high free energy barrier for the anions, they could not penetrate the (7, 7) CNT.

Fig. 3 shows the current-electrical field profile. It was observed that the current increased linearly along with the application of electrical field. By fitting a linear regression to the current-electrical field curve, sodium conductance was calculated to be 128.2 pS in the (7, 7) CNT and chloride conductance was calculated to be 421.3 pS in the (8, 8) CNT.

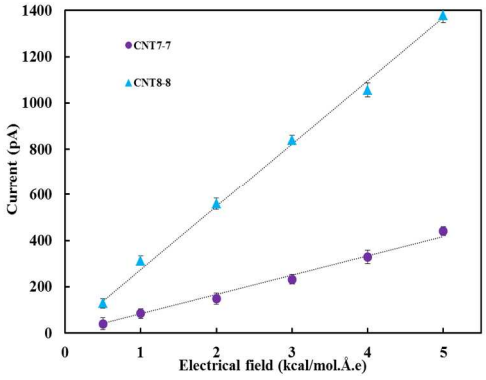

Fig.3 Current-electrical field curve for Na+ ion in the (7, 7) CNT and Cl- ion in the (8, 8) CNT; lines have been obtained from a linear regression. Each data point represents the average of six sets of simulations.

Also, the number of selective ions and water molecules passing through CNTs increased linearly with the application of the electrical field which is depicted in Fig. 4.

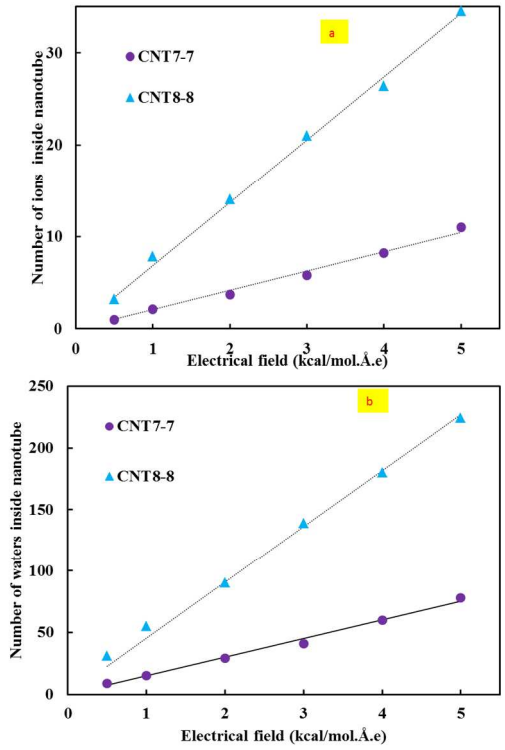

Fig.4 (a) The number of ions passing through the CNTs: Na+ ion from the (7, 7) CNT and Cl- ion from the (8, 8) CNT; (b) the number of water molecules passing through the CNTs. Lines have been obtained from a linear regression.

The transport rate of the water molecules (TRW) through the CNTs is defined as the ratio of the average number of passing water molecules to the simulation time. Fig. 5 shows that the TRW for the (8, 8) CNT is greater than the (7, 7) CNT which is due to the larger radius of the (8, 8) CNT.

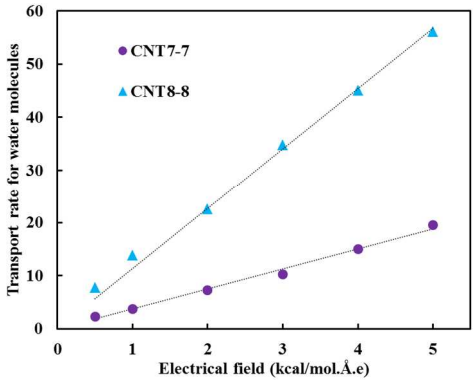

Fig.5 Transport rate for water molecules through the CNTs.

Fig. 6 shows the normalized TRW with respect to the number of transported ions. These results substantiate that the normalized TRW (transported water for one permeated ion) was almost independent of the applied electrical field.

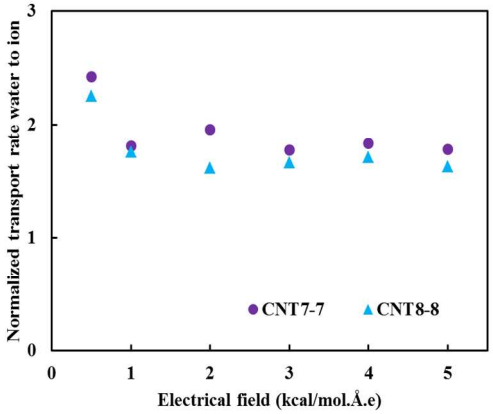

Fig.6 The Normalized transport rate water with respect to the number of transported ion.

Also, as it can be seen in this Fig., this parameter in the (7, 7) CNT is larger than that of the (8, 8) CNT. This trend indicated that with respect to each ion passing through the CNT, more water molecules passed through the (7, 7) CNT in comparison to the (8, 8) CNT. This phenomenon also acknowledged that in the radial distribution function (RDF), the peak intensity of sodium ion is higher than that of chloride.

Fig. 7(a) demonstrates the number of hydrogen bonds inside the CNTs under the application of the electrical fields. In this system, the number of hydrogen bonds increases as the applied electrical field increases. Since the applied electrical field increases, more water passes through the CNTs. It should be noted that the magnitude of increase in the (8, 8) CNT is higher than that of the (7, 7) CNT which is attributed to the large radius of the (8, 8) CNT. Another parameter which confirmed this trend is the time average of the normalized hydrogen bonds with respect to the number of inner water molecules in the applied electrical fields (see Fig. 7(b)). As it was hypothesized, this parameter also increases by increasing the applied electrical field. The average density of water inside the CNTs over 4 ns simulation (see Fig. 8) also confirmed this trend.

Table 2 displays the retention time of ions which is equal to the time of passing one ion through the nanotube as a function of the applied electrical field.

Table2. Retention time of ions in the applied electrical fields.

Electrical field (kcal.mol^{-1}.Å^{-1}.e^{-1})	**Retention time of ions (ns)**	
	Na^+ in (7,7) CNT	Cl^- in (8,8) CNT
0.5	1.996	1.532
1	1.136	0.451
2	0.583	0.267
3	0.258	0.097
4	0.071	0.050
5	0.0108	0.0111

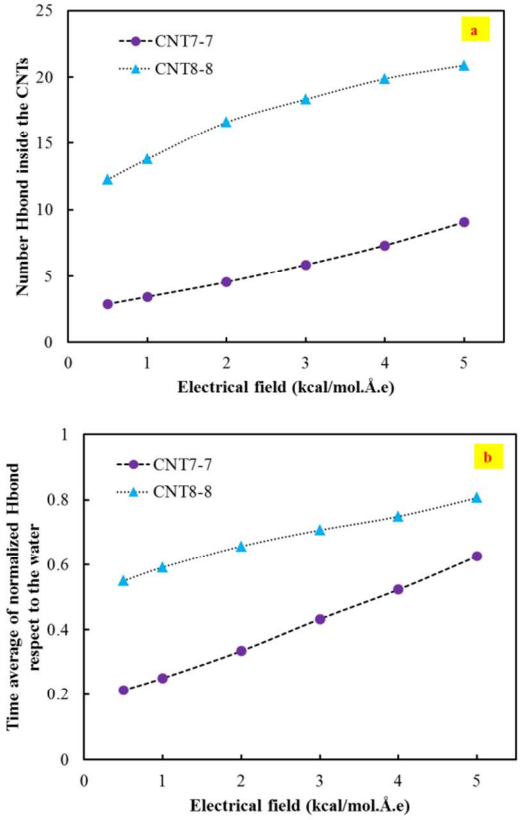

Fig.7 (a) The number of hydrogen bonds inside the CNTs in the applied electrical fields; (b) The time average of the normalized hydrogen bonds with respect to the number of inner water molecules.

The amount of time will be less if ions pass fast through CNTs and this will speed up water desalination. This Table shows that the larger the electrical fields, the smaller the retention time. As it might be expected, the retention time of ions is larger for sodium ions in the (7, 7) CNT than that of chlorine ions in the (8, 8) CNT. Given the PMF curves, it can be observed that sodium ions, when compared with chloride ions are more inclined to stay in the potential well. This is why the rate of permeation of sodium ions was less than that of chlorine. Moreover, these ions spend more time inside the (7, 7) CNT.

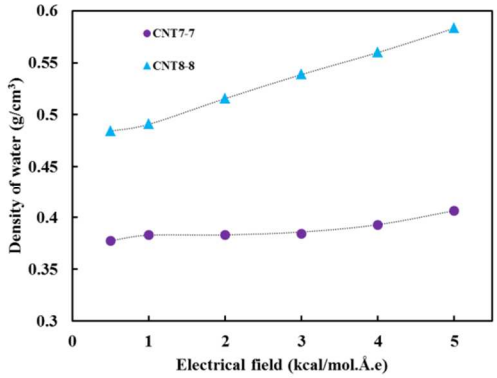

Fig.8 The average density of water inside the CNTs in the applied electrical fields.

To describe the structure of each ion in the simulation box, the researchers calculated the RDF from the trajectories files. Fig. 9 represents the RDF between ions and water molecules under the applied electrical fields. Due to the repulsive forces between atom types, at a short distance, RDF is zero. The locations of the maximum and minimum of the peaks were similar in all electrical fields. However, the intensity of the peaks was different in each electrical field which indicates the change in the hydration number of the ions (sodium or chlorine) in each electrical field. Intense first peaks of RDFs can be considered as an evidence of the formation of the well-pronounced first coordination (solvation) shell around the ions.

Fig. 9(a) displays sodium-water RDF inside the (7, 7) CNTs while Fig. 9(b) illustrates RDFs of chlorine-water inside the (8, 8) CNTs. As shown in these Figs., peak intensity changes by changing the applied electric field. This behaviour can be explained by the retention time of ions. Under lower electrical fields, ion spends extra time in its hydration shell; That is, it has longer retention time; therefore, the ion-water RDF would be intensified. A close examination of Table 2 and Figs. 9 reveals that the order of RDF for ions is the same as that of retention times. In other words, the RDF with a higher peak corresponds to the larger retention time. Furthermore, RDFs show broad second peaks with similar intensities. This indicates that the second hydration shells of the ions can be identified but they are not defined as the first hydration shell.

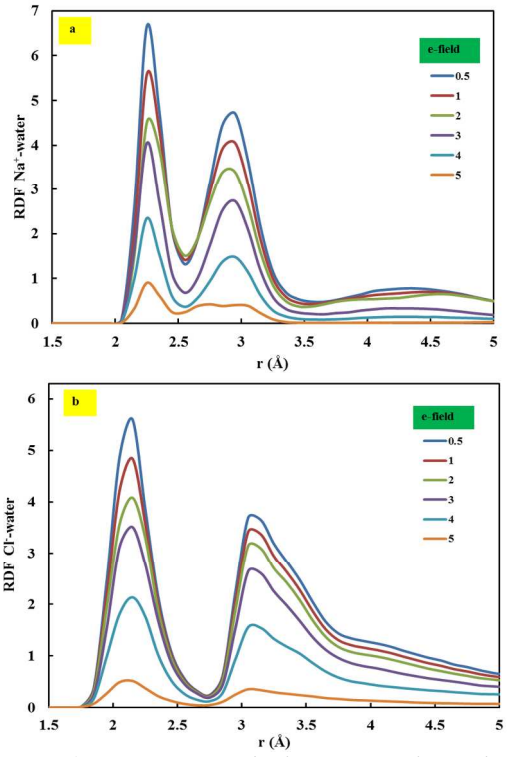

Fig.9 RDF for ion-water inside the CNTs at the applied electrical fields: (a) (7, 7) CNT; (b) (8, 8) CNT.

Fig. 10 illustrates the z position of Na^+ during the simulation time under low and high electric fields. As shown in this Fig., there is an overlap between the retention times of ions in the lower electrical field but there is no overlap in the higher electrical fields.

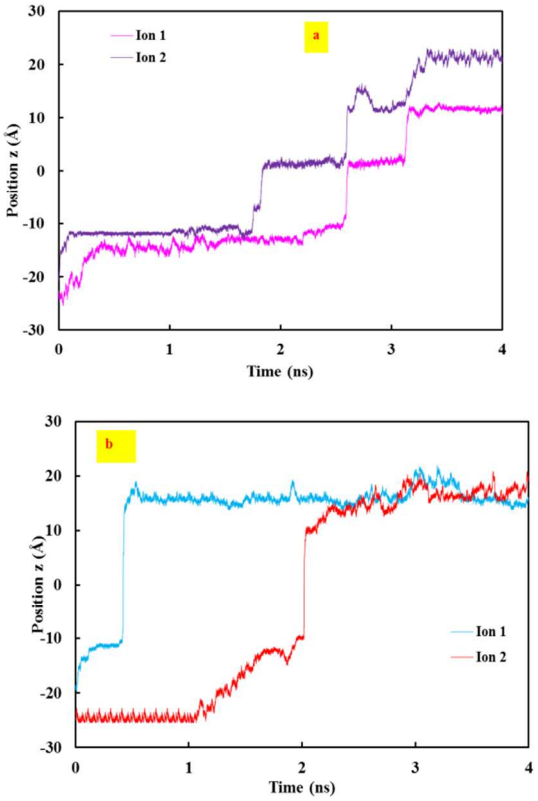

Fig.10 The z position of Na^+ during the simulation time (a) in the lower electrical field; (b) in the higher electrical field.

In other words, under the application of lower electric fields, one ion gets into the CNT and does not get out of it until a second ion enters. However, under a higher electric field, ions cross CNT without the assistance of other ions.

In the present study, the researchers made an attempt to explain the time evolutions under the applied electrical field in the water molecules. In doing so, the time variations of the force applied on the particles (as the electrical field) in the simulation were utilized. At the outset of the simulation, as a consequence of the deviation of the system from the equilibrium, these force components (such as other thermodynamic and mechanical quantities) have relatively large fluctuations with values which move towards optimum values. These values are directed by the integration or optimization algorithm. The applied forces on the particles are accompanied by other factors (band, angle, electrostatic and coulomb forces) have been treated by the solving the equations of movement and integration with respect to time. As the simulation runs and system goes to the equilibrium state, the magnitude of the applied electrical field approaches the optimal, equilibrium value during the simulation and their thermodynamic values are regarded as the average value at the simulation time period.

4. Conclusions

For desalinating water, a series of a series of MD simulations were conducted to investigate the ion selective permeation events through (7, 7) and (8, 8) CNTs. The results of MD simulations indicated that ion selectivity was realized by CNTs under the effect of using electrical field. The results of the study revealed that one Na^+ ion entered the (7, 7) CNT and managed to go through the entire length of the nanotube and then get out of it. In contrast, the Cl^- ions were not able to even enter the (7, 7) CNT. In the case of the (8, 8) CNT, the opposite phenomenon occurred. Indeed, it can be argued that the simplicity of CNT structure was a significant advantage for manufacturing an ion-selective nanodevice. It can be concluded that the application of electrical field can have an impact on the following properties of the studied systems: PMF, the ionic current, ion retention time, water density, TRW and RDF. Eventually, it can be maintained that the results of the study highlight the capability of the CNTs with respect to water desalination technology.

Acknowledgements

Authors thank the Azarbaijan Shahid Madani University and Iranian Nanotechnology Initiative Council for their support.

Notes and references

1. M. L. Davis, *Water and wastewater engineering: design principles and practice*, McGraw-Hill, New York, 2011.
2. N. K. Shammas and L. K. Wang, *Water and wastewater engineering: water supply and wastewater removal*, Wiley, Hoboken, 2011.
3. R. L. Droste, *Theory and practice of water and wastewater treatment*, J. Wiley, New York, 1997.
4. A. Thess, R. Lee, P. Nikolaev, H. Dai, P. Petit, J. Robert, C. Xu, Y. H. Lee, S. G. Kim, A. G. Rinzler, D. T. Colbert, G. E. Scuseria, D. Tománek, J. E. Fischer and R. E. Smalley, *Science*, 1996, 273, 483-487.
5. B. Corry, *J. Phys. Chem. B*, 2008, 112, 1427-1434.
6. S. Iijima, *Nature*, 1991, 354, 56-58.
7. J.-Y. Guo, C.-X. Xu, F.-Y. Sheng, Z.-L. Jin, Z.-L. Shi, J. Dai and Z.-H. Li, *Quat. Matt.*, 2013, 2, 181-186.
8. M. Meyyappan, *Carbon nanotubes: science and applications*, CRC press, 2004.
9. S. Kar, R. C. Bindal and P. K. Tewari, *Nano Today*, 2012, 7, 385-389.
10. M. S. Dresselhaus, G. Dresselhaus and P. Avouris, *Carbon nanotubes: synthesis, structure, properties, and applications*, Springer, New York, 2001.
11. M. Endo, S. Iijima and M. S. Dresselhaus, *Carbon nanotubes*, Pergamon, Oxford, 1st edn., 1996.
12. J. Azamat and J. Sardroodi, *Monatsh Chem*, 2014, 145, 881-890.
13. J. J. Sardroodi, J. Azamat, A. Rastkar and N. R. Yousefnia, *Chem. Phys.*, 2012, 403, 105-112.
14. B. Corry, *Energy Environ. Sci.*, 2011, 4, 751-759.
15. D. A. Doshi, N. K. Huesing, M. Lu, H. Fan, Y. Lu, K. Simmons-Potter, B. G. Potter, A. J. Hurd and C. J. Brinker, *Science*, 2000, 290, 107-111.
16. D. Stein, M. Kruithof and C. Dekker, *Phys. Rev. Lett.*, 2004, 93, 035901.
17. K. Leung, S. B. Rempe and C. D. Lorenz, *Phys. Rev. Lett.*, 2006, 96, 095504.
18. P. S. Goh, A. F. Ismail and B. C. Ng, *Desalination*, 2013, 308, 2-14.
19. C. H. Ahn, Y. Baek, C. Lee, S. O. Kim, S. Kim, S. Lee, S.-H. Kim, S. S. Bae, J. Park and J. Yoon, *J. Ind. Eng. Chem.*, 2012, 18, 1551-1559.
20. A. Kalra, S. Garde and G. Hummer, *PNAS*, 2003, 100, 10175-10180.
21. A. Waghe, J. C. Rasaiah and G. Hummer, *J. Chem. Phys.*, 2002, 117, 10789-10795.
22. C. F. Lopez, S. O. Nielsen, P. B. Moore and M. L. Klein, *PNAS*, 2004, 101, 4431-4434.

23. R. Das, M. E. Ali, S. B. A. Hamid, S. Ramakrishna and Z. Z. Chowdhury, *Desalination*, 2014, 336, 97-109.
24. C. Y. Lee, W. Choi, J.-H. Han and M. S. Strano, *Science*, 2010, 329, 1320-1324.
25. T. A. Hilder, D. Gordon and S.-H. Chung, *Biophys. J.*, 2010, 99, 1734-1742.
26. M. E. Suk, A. V. Raghunathan and N. R. Aluru, *Appl. Phys. Lett.*, 2008, 92.
27. F. Fornasiero, H. G. Park, J. K. Holt, M. Stadermann, C. P. Grigoropoulos, A. Noy and O. Bakajin, *PNAS*, 2008, 105, 17250-17255.
28. M. Majumder, N. Chopra, R. Andrews and B. J. Hinds, *Nature*, 2005, 438, 44-44.
29. M. K. Tsai, J. L. Kuo and J. M. Lu, *Phys. Chem. Chem. Phys.*, 2012, 14, 13402-13408.
30. M. W. Schmidt, K. K. Baldridge, J. A. Boatz, S. T. Elbert, M. S. Gordon, J. H. Jensen, S. Koseki, N. Matsunaga, K. A. Nguyen, S. Su, T. L. Windus, M. Dupuis and J. A. Montgomery, *J. Comput. Chem.*, 1993, 14, 1347-1363.
31. L. Kalé, R. Skeel, M. Bhandarkar, R. Brunner, A. Gursoy, N. Krawetz, J. Phillips, A. Shinozaki, K. Varadarajan and K. Schulten, *J. Comput. Phys.*, 1999, 151, 283-312.
32. W. Humphrey, A. Dalke and K. Schulten, *J. Mol. Graphics*, 1996, 14, 33-38.
33. J. Azamat and J. J. Sardroodi, *Journal of Computational and Theoretical Nanoscience*, 2014, 11, 2611-2617.
34. J. Azamat, J. J. Sardroodi and A. Rastkar, *Desalin. Water Treat.*, 2014, 1-9.
35. J. Azamat, A. Khataee and S. Joo, *J. Mol. Model.*, 2014, 20, 1-9.
36. J. Azamat, A. Khataee and S. W. Joo, *J. Mol. Graphics Modell.*, 2014, 53, 112-117.
37. R. J. Mashl, S. Joseph, N. R. Aluru and E. Jakobsson, *Nano Lett.*, 2003, 3, 589-592.
38. Y. Shim, Y. Jung and H. J. Kim, *Phys. Chem. Chem. Phys.*, 2011, 13, 3969-3978.
39. T. Darden, D. York and L. Pedersen, *J. Chem. Phys.*, 1993, 98, 10089-10092.
40. J. K. Holt, H. G. Park, Y. Wang, M. Stadermann, A. B. Artyukhin, C. P. Grigoropoulos, A. Noy and O. Bakajin, *Science*, 2006, 312, 1034-1037.
41. B. J. Hinds, N. Chopra, T. Rantell, R. Andrews, V. Gavalas and L. G. Bachas, *Science*, 2004, 303, 62-65.
42. A. Bala Subramaniam, M. Abkarian, L. Mahadevan and H. A. Stone, *Nature*, 2005, 438, 930-930.
43. T. A. Hilder, D. Gordon and S.-H. Chung, *Small*, 2009, 5, 2183-2190.
44. T. A. Hilder, R. Yang, D. Gordon, A. P. Rendell and S.-H. Chung, *J. Phys. Chem. C*, 2012, 116, 4465-4470.
45. X. Gong, J. Li, K. Xu, J. Wang and H. Yang, *J. Am. Chem. Soc.*, 2010, 132, 1873-1877.
46. J. Su and H. Guo, *J. Phys. Chem. B*, 2012, 116, 5925-5932.
47. J. C. Phillips, R. Braun, W. Wang, J. Gumbart, E. Tajkhorshid, E. Villa, C. Chipot, R. D. Skeel, L. Kalé and K. Schulten, *J. Comput. Chem.*, 2005, 26, 1781-1802.
48. W. L. Jorgensen, J. Chandrasekhar, J. D. Madura, R. W. Impey and M. L. Klein, *J. Chem. Phys.*, 1983, 79, 926-935.
49. A. D. MacKerell, D. Bashford, Bellott, R. L. Dunbrack, J. D. Evanseck, M. J. Field, S. Fischer, J. Gao, H. Guo, S. Ha, D. Joseph-McCarthy, L. Kuchnir, K. Kuczera, F. T. K. Lau, C. Mattos, S. Michnick, T. Ngo, D. T. Nguyen, B. Prodhom, W. E. Reiher, B. Roux, M. Schlenkrich, J. C. Smith, R. Stote, J. Straub, M. Watanabe, J. Wiórkiewicz-Kuczera, D. Yin and M. Karplus, *J. Phys. Chem. B*, 1998, 102, 3586-3616.
50. I. S. Joung and T. E. Cheatham, *J. Phys. Chem. B*, 2008, 112, 9020-9041.
51. R. Kjellander and H. Greberg, *J. Electroanal. Chem.*, 1998, 450, 233-251.
52. S. Kumar, P. W. Payne and M. Vásquez, *J. Comput. Chem.*, 1996, 17, 1269-1275.

Table of Contents Graphic

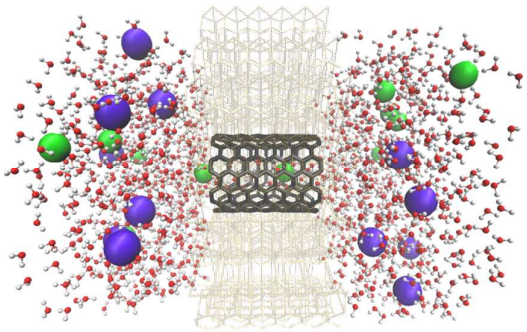

Separation of ions from water using armchair carbon nanotubes